Available online at www.sciencedirect.com
SCIENCE DIRECT®
Journal of Sound and Vibration 276 (2004) 511–525
JOURNAL OF SOUND AND VIBRATION
www.elsevier.com/locate/jsvi

Mode shapes and stress-resultants of circular Mindlin plates with free edges

C.M. Wang[a], Y. Xiang[b,*], E. Watanabe[c], T. Utsunomiya[c]

[a] *Department of Civil Engineering, National University of Singapore, Kent Ridge, Singapore 119260*
[b] *School of Engineering and Industrial Design, Centre for Construction Technology and Research, University of Western Sydney, Penrith South DC, NSW 1797, Australia*
[c] *Department of Civil Engineering, Kyoto University, Kyoto, Japan*

Received 10 October 2002; accepted 4 August 2003

Abstract

Presented herein are exact vibration mode shapes and modal stress-resultants for freely vibrating, circular Mindlin plates with free edges. These documented solutions are important in the hydroelastic analysis of very large circular floating structures (VLFS) which are commonly modeled as plates with free edges. The exact vibration solutions will enable engineers to obtain a very accurate set of deflections and stress-resultants for circular VLFS under the action of waves. Such benchmark results will allow engineers and researchers to ascertain the accuracy of whatever numerical techniques that are eventually proposed for predicting accurate hydroelastic responses of arbitrarily shaped VLFS.

1. Introduction

In the hydroelastic analysis of very large floating structures such as the one shown in Fig. 1, the pontoon-type structures are often modeled as huge plates with free edges [1–3]. The analysis consists of separating the hydrodynamic analysis from the dynamic response analysis of the very large circular floating structures (VLFS). The deflection of the plate is decomposed into vibration modes. Then the hydrodynamic radiation forces are evaluated for unit amplitude motions of each mode. A numerical method, such as the Galerkin's method (by which the governing equation of the plate is approximately satisfied), is used to determine the modal amplitudes. The modal responses are then summed up to obtain the total response.

*Corresponding author. Tel.: +61-2-4736-0395; fax: +61-2-4736-0833.
E-mail addresses: cvewcm@nus.edu.sg (C.M. Wang), y.xiang@uws.edu.au (Y. Xiang).

0022-460X/$ - see front matter © 2003 Elsevier Ltd. All rights reserved.
doi:10.1016/j.jsv.2003.08.010

Fig. 1. A sewage treatment plant on a circular VLFS (Courtesy of the Floating Structures Association of Japan).

Recently, Wang et al. and Xiang et al. [4,5] showed that the use of the classical thin plate theory for modelling the pontoon-type VLFS and well-known numerical methods (such as the Ritz method and the finite element method) for vibration analysis yields modal stress-resultants that: (a) do not satisfy the natural boundary conditions and (b) contain oscillations/ripples in their distributions, casting doubts on the accuracy of their peak values. When these modal solutions are used in the hydrodynamic analysis, the final stress-resultants will contain these aforementioned inaccuracies.

Wang et al. [6,7] proposed some remedies for the problem that involve the use of the more refined Mindlin plate theory (that incorporates the effects of transverse shear deformation and rotary inertia), thereby improving on the accuracy of the stress-resultants, especially the transverse shear forces and twisting moments. Moreover, the remedies involve adding penalty functions to the energy functional to enforce the satisfaction of the natural boundary conditions as well as using a post-processing smoothing technique to erase the oscillations. However, in order to really assess how good these proposed remedies, one needs exact solutions to serve as benchmark checks. Prompted by this need, the authors recognize that exact solutions can be obtained for circular plates with free edges. Although exact vibration frequencies for circular plates with free edges are already available in the literature [8,9], their corresponding modal stress-resultants are hitherto not available. Thus, the aim of this study is to document the exact mode shapes and modal stress-resultants for circular Mindlin plates so that researchers may readily use them in the hydroelastic analysis of circular VLFS. The accurate deflections and stress-resultants of such circular VLFS will be extremely valuable to ascertain the accuracy of whatever numerical techniques that are eventually proposed for predicting accurate hydroelastic responses of arbitrarily shaped VLFS under the action of waves.

2. Mathematical modelling

Consider an isotropic, flat circular plate of radius R, thickness h, mass density ρ, the Poisson ratio v, Young's modulus E and shear modulus $G\ (= E/[2(1+v)])$. The plate is free from any attachment/support as shown in Fig. 2. The problem at hand is to determine the modal displacement fields and stress-resultants for the freely vibrating circular plate. The modelling of the plate is based on the Mindlin shear deformable plate theory [10]. The obtained modal displacements and stress-resultants may be used for the analysis and design of VLFS circular structures.

Although the exact analysis of vibration of circular Mindlin plates was carried out by previous researchers [8,9], the mathematical modelling of the analysis is briefly presented herein for readers' easy reference. Mindlin and Deresiewicz [8] cleverly proposed that the displacement fields of the plate may be expressed as functions of three potentials Θ_1, Θ_2 and Θ_3:

$$\psi_r = (\sigma_1 - 1)\frac{\partial \Theta_1}{\partial \chi} + (\sigma_2 - 1)\frac{\partial \Theta_2}{\partial \chi} + \frac{1}{\chi}\frac{\partial \Theta_3}{\partial \theta}, \tag{1}$$

$$\psi_\theta = (\sigma_1 - 1)\frac{1}{\chi}\frac{\partial \Theta_1}{\partial \theta} + (\sigma_2 - 1)\frac{1}{\chi}\frac{\partial \Theta_2}{\partial \theta} - \frac{\partial \Theta_3}{\partial \chi}, \tag{2}$$

$$\bar{w} = \Theta_1 + \Theta_2, \tag{3}$$

where

$$\sigma_1, \sigma_2 = \frac{(\delta_2^2, \delta_1^2)}{\left[\dfrac{\tau^2\lambda^2}{12} - \dfrac{6(1-v)\kappa^2}{\tau^2}\right]} = \frac{2(\delta_2^2, \delta_1^2)}{\delta_3^2(1-v)}, \tag{4}$$

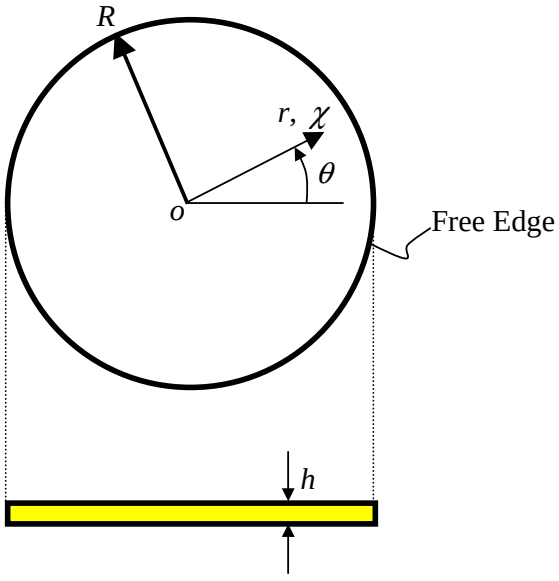

Fig. 2. Geometry and the polar co-ordinates system of a circular Mindlin plate.

$$\delta_1^2, \delta_2^2 = \frac{\lambda^2}{2}\left[\frac{\tau^2}{12} + \frac{\tau^2}{6(1-\nu)\kappa^2} \pm \sqrt{\left(\frac{\tau^2}{12} - \frac{\tau^2}{6(1-\nu)\kappa^2}\right)^2 + \frac{4}{\lambda^2}}\right], \tag{5}$$

$$\delta_3^2 = \frac{2}{(1-\nu)}\left[\frac{\tau^2\lambda^2}{12} - \frac{6(1-\nu)\kappa^2}{\tau^2}\right], \tag{6}$$

$$\bar{w} = \frac{w}{R}, \quad \chi = \frac{r}{R}, \quad \tau = \frac{h}{R}, \quad \lambda = \omega R^2\sqrt{\frac{\rho h}{D}} \tag{7}$$

in which r and θ are the radial and circumferential co-ordinates of the polar co-ordinate system, w, ψ_r and ψ_θ the transverse displacement and rotations in the Mindlin plate theory, $\bar{w}$ is the non-dimensionalized transverse displacement of the plate, χ the non-dimensionalized radial co-ordinate (see Fig. 2), κ^2 the shear correction factor, and λ the angular frequency parameter.

Based on these potentials, the governing differential equations of the vibrating circular plate, in polar co-ordinates, may be transformed into three harmonic equations. The solutions of the three harmonic equations can be expressed as

$$\Theta_1 = A_1 R_n(\Delta_1\chi)\cos n\theta, \quad \Theta_2 = A_2 R_n(\Delta_2\chi)\cos n\theta, \quad \Theta_3 = A_3 R_n(\Delta_3\chi)\sin n\theta, \tag{8}$$

where

$$\Delta_j = \begin{cases} \delta_j & \text{if } \delta_j^2 \geqslant 0, \\ \mathrm{Im}(\delta_j) & \text{if } \delta_j^2 < 0, \end{cases} \quad j = 1, 2, 3, \tag{9}$$

$$R_n(\Delta_j\chi) = \begin{cases} \mathrm{J}_n(\Delta_j\chi) & \text{if } \delta_j^2 \geqslant 0, \\ \mathrm{I}_n(\Delta_j\chi) & \text{if } \delta_j^2 < 0, \end{cases} \quad j = 1, 2, 3 \tag{10}$$

in which A_j ($j = 1$, 2 and 3) are the arbitrary constants that will be determined by the free boundary conditions of the plate, n is the number of nodal diameters of a vibration mode, and $\mathrm{J}_n(\cdot)$ and $\mathrm{I}_n(\cdot)$ are the first kind and the modified first kind Bessel functions of order n.

The periphery conditions of a free circular Mindlin plate at the edge are defined as follows

$$Q_r = \kappa^2 Gh\left(\frac{\partial\bar{w}}{\partial\chi} + \psi_r\right) = 0, \quad M_{rr} = \frac{D}{R}\left[\frac{\partial\psi_r}{\partial\chi} + \frac{\nu}{\chi}\left(\psi_r + \frac{\partial\psi_\theta}{\partial\theta}\right)\right] = 0,$$

$$M_{r\theta} = \frac{D}{R}\left(\frac{1-\nu}{2}\right)\left[\frac{1}{\chi}\left(\frac{\partial\psi_r}{\partial\theta} - \psi_\theta\right) + \frac{\partial\psi_\theta}{\partial\chi}\right] = 0. \tag{11}$$

The displacement fields and the stress-resultants of the circular plate may be expressed in terms of the arbitrary constants A_j, $j = 1$, 2 and 3 [8,9,11]. In view of Eqs. (1)–(3) and (8), a homogeneous system of equations can be derived by implementing the free boundary conditions of the plate along the circular edge [Eq. (11)]

$$\mathbf{K}\begin{Bmatrix} A_1 \\ A_2 \\ A_3 \end{Bmatrix} = \{\mathbf{0}\}, \tag{12}$$

and **K** is a 3×3 matrix. The angular frequency ω of the plate is evaluated by setting the determinant of **K** in Eq. (12) to be zero.

The modal displacement fields w, ψ_r and ψ_θ and modal stress-resultants Q_r, M_{rr} and $M_{r\theta}$ are calculated after the angular frequency ω and the corresponding eigenvector $[A_1\ A_2\ A_3]^{\mathrm{T}}$ are obtained. The maximum transverse displacement of the plate in vibration is normalized by setting

$$\left|\frac{w_{max}}{R}\right| = |\bar{w}_{max}| = 1, \tag{13}$$

and the corresponding modal stress-resultants are presented in their non-dimensional forms as follows

$$\bar{Q}_r = \frac{R^2}{D} Q_r, \quad \bar{M}_{rr} = \frac{R}{D} M_{rr}, \quad \bar{M}_{r\theta} = \frac{R}{D} M_{r\theta}. \tag{14}$$

3. Results and discussions

The Poisson ratio $\nu = 0.3$ and the shear correction factor $\kappa^2 = \frac{5}{6}$ are adopted for all calculations. Exact vibration frequency parameters $\lambda = \omega R^2\sqrt{\rho h/D}$ for free circular Mindlin plates are presented in Table 1. The number of nodal diameters n varies from 1 to 4 and the mode sequence number s for a given n value changes from 1 to 4, respectively.

In the hydrodynamic analysis of a VLFS structure, the mode shapes and modal stress-resultants from the free vibration analysis of the structure are utilized to predict the dynamic responses of the structure. The exact mode shapes and modal stress-resultants for free circular Mindlin plates are presented herein, thus serve as important benchmark values for researchers to verify their numerical models for circular Mindlin plate analysis. The cases in Table 1 that are highlighted by boldfacing the values have their modal shapes and modal stress-resultants depicted in Figs. 3 and 4, respectively. Note that the modal displacement fields and modal stress-resultants in Figs. 3 and 4 are plotted along radial direction where their peak values are found. The modal displacements $\bar{w}$ and ψ_r, and modal stress-resultants $\bar{Q}_r$ and $\bar{M}_{rr}$ in the circumferential direction vary with $\cos n\theta$, while the modal displacement ψ_θ and modal stress-resultant $\bar{M}_{r\theta}$ vary with $\sin n\theta$.

Figs. 3a and 4a present the normalized modal displacement fields and modal stress-resultants along the radial direction for a thinner circular Mindlin plate ($h/R = 0.01$) and a thicker plate ($h/R = 0.10$), respectively. The plates vibrate in axisymmetric modes ($n = 0$). The modal displacement fields and modal stress-resultants for the thinner and thicker plates show very similar trends. The values of the modal rotation ψ_r and the modal stress-resultants $\bar{Q}_r$ and $\bar{M}_{rr}$ for the thicker plate are smaller than the ones for the thinner plate. As expected, the rotation ψ_θ and moment $\bar{M}_{r\theta}$ on the whole plate and the rotation ψ_r and shear force $\bar{Q}_r$ at the centre of the plates ($\chi = r/R = 0$) are zero due to the plates vibrating in axisymmetric modes. The modal stress-resultants $\bar{Q}_r$, $\bar{M}_{rr}$ and $\bar{M}_{r\theta}$ vanish at the plate free edge ($\chi = r/R = 1$). The number of nodal circumferential lines of the modal displacements $\bar{w}$ and ψ_r and modal stress-resultant $\bar{M}_{rr}$ increases from 1 to 4 as the mode sequence number s varies from 1 to 4. However, the number of nodal circumferential lines of the modal stress-resultant $\bar{Q}_r$ changes from 2 to 5 while the mode sequence number s increases from 1 to 4.

Table 1
Frequency parameters $\lambda = \omega R^2\sqrt{\rho h/D}$ for free circular Mindlin plates ($\nu = 0.3$, $\kappa^2 = 5/6$)

n	s	Thickness ratio, h/R				
		0.005	0.01	0.10	0.15	0.20
0	1	9.00279	**9.00175**	**8.86877**	8.71132	8.50800
0	2	38.4365	**38.4164**	**36.0592**	33.7076	31.1562
0	3	87.7151	**87.6099**	**76.7577**	67.9521	59.7944
0	4	156.706	**156.370**	**126.483**	106.673	90.3596
1	1	20.4698	20.4613	19.7165	18.9273	17.9939
1	2	59.7918	59.7396	54.2993	49.4103	44.5225
1	3	118.889	118.692	100.071	86.4264	74.5493
1	4	197.689	197.151	153.044	126.415	105.419
2	1	5.35655	**5.35453**	**5.27822**	5.20584	5.11560
2	2	35.2426	35.2140	33.0500	30.9716	28.7085
2	3	84.3196	84.2088	73.9519	65.6276	57.8636
2	4	153.183	152.848	123.973	104.738	88.8221
3	1	12.4320	**12.4237**	**12.0667**	11.7271	11.3209
3	2	52.9684	52.9040	48.2623	44.1745	40.0346
3	3	111.856	111.655	94.6541	82.1058	71.0638
3	4	190.492	189.964	148.269	122.837	102.640
4	1	21.8188	**21.7983**	**20.8089**	19.8850	18.8351
4	2	73.4713	73.3521	64.9534	58.1397	51.6622
4	3	142.283	141.953	116.137	98.6884	84.0671
4	4	230.727	229.944	172.818	140.694	116.017

Note: n is the number of nodal diameters of the mode and s is the mode sequence for a given n value. The cases with the boldfaced values have their modes and modal stress-resultants presented.

Figs. 3b and 4b show the normalized modal displacement fields and modal stress-resultants along the radial direction for a thinner circular Mindlin plate ($h/R = 0.01$) and a thicker plate ($h/R = 0.10$), respectively. The vibration of the plates is non-axisymmetric. Similar trends are observed for the modal displacement fields and modal stress-resultants of the thinner and thicker plates. The values of the modal displacements ψ_r and ψ_θ and the modal stress-resultants $\bar{Q}_r$ and $\bar{M}_{rr}$ for the thicker plate are smaller than the ones for the thinner plate. The mode sequence number s is fixed at 1 and the number of nodal diameters n varies from 1 to 4. It is interesting to observe that there are two nodal circumferential lines for the modal displacement $\bar{w}$ if the plates vibrate with one nodal diameter ($n = 1$). The modes with two nodal diameters ($n = 2$) are the fundamental modes as shown by the frequency values in Table 1. The modal displacement fields and stress-resultants for the modes with 3 and more nodal diameters (i.e. $n \geqslant 3$) show similar trends in general. The modal displacement fields $\bar{w}$, ψ_r and ψ_θ and stress-resultants $\bar{Q}_r$, $\bar{M}_r$ and $\bar{M}_{r\theta}$ are zero at the centre of the plates ($\chi = r/R = 0$). The values of the displacement fields $\bar{w}$, ψ_r and ψ_θ increase monotonically with increasing radial co-ordinate ($\chi = r/R$) except for the rotation ψ_θ of the thicker plate near the free edge where a slight decrease of ψ_θ is observed. The stress-resultants $\bar{Q}_r$, $\bar{M}_{rr}$ and $\bar{M}_{r\theta}$ vanish at the plate free edge for all cases shown in Figs. 3b and 4b. It is noted that for the thinner plate ($h/R = 0.01$), there are sharp variations in stress-resultants $\bar{Q}_r$ and $\bar{M}_{r\theta}$ near the vicinity of the free edge when the number of nodal diameters n varies from 2 to 4.

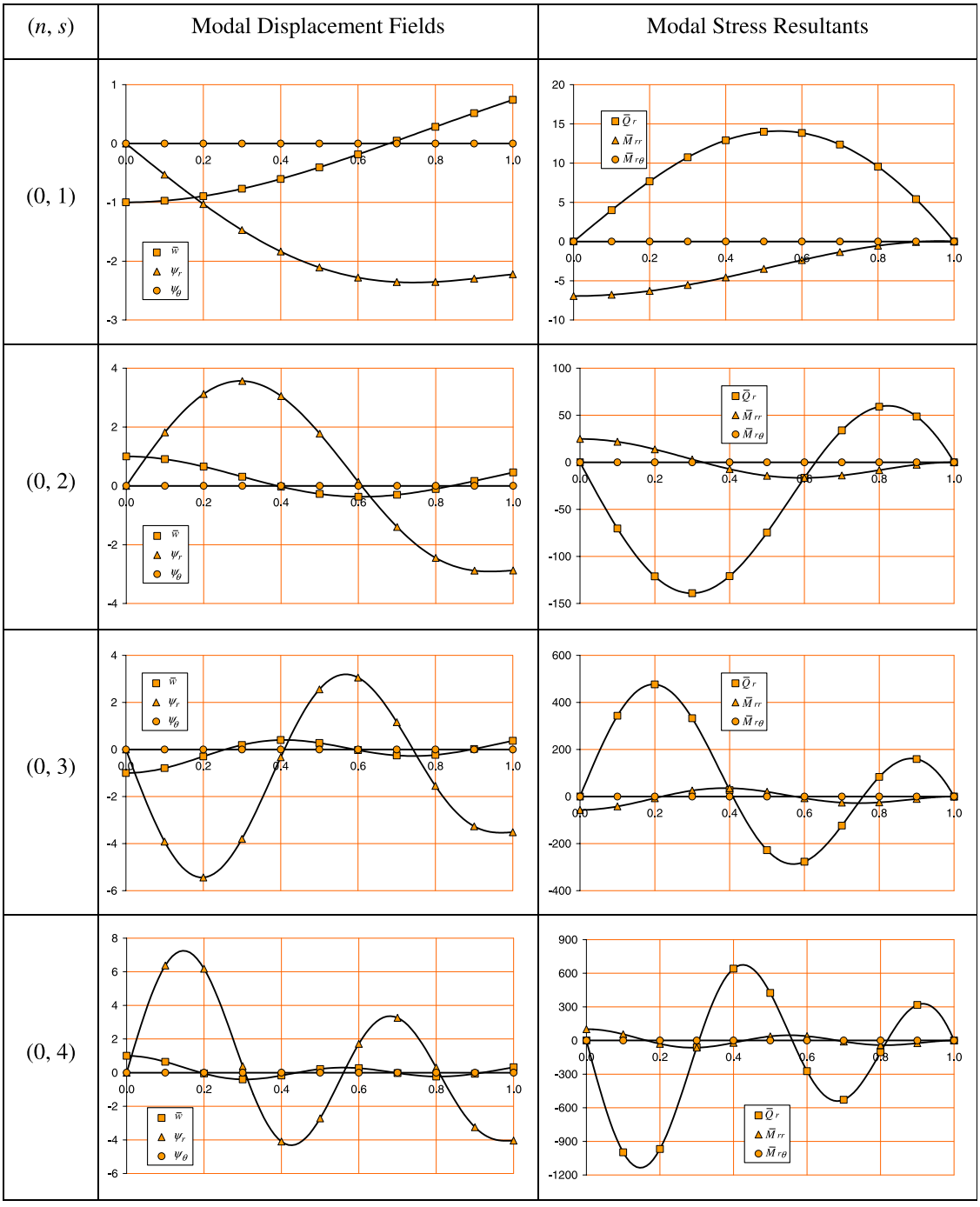

(a)

Fig. 3. (a) Mode shapes and modal stress-resultants for free circular Mindlin plates with thickness ratio $h/R = 0.01$. The number of nodal diameters $n = 0$ (axisymmetric modes). (b) Mode shapes and modal stress-resultants for free circular Mindlin plates with thickness ratio $h/R = 0.01$. The number of nodal diameters is $n = 1$, 2, 3 and 4, respectively.

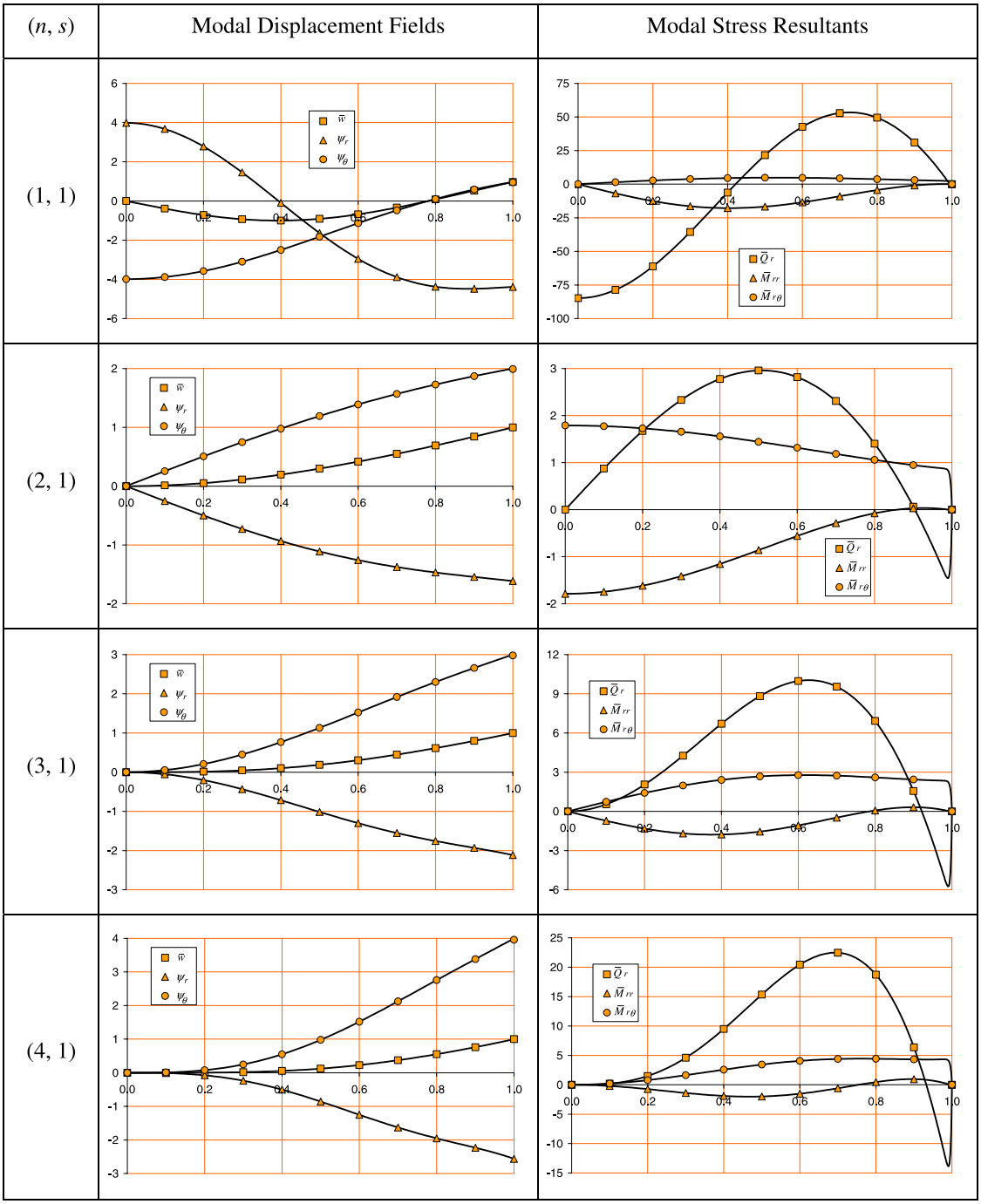

(b)

Fig. 3 (*continued*).

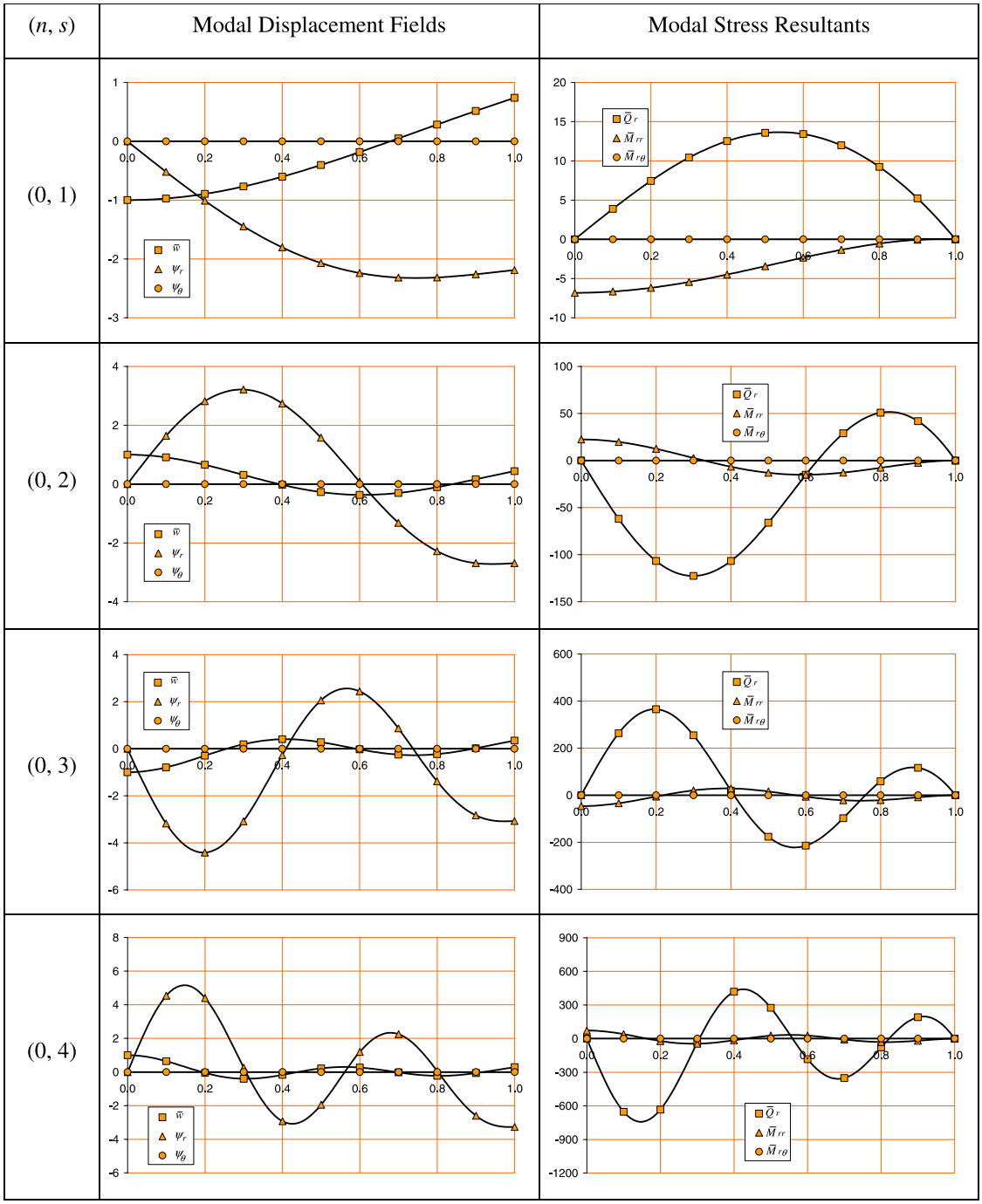

(a)

Fig. 4. (a) Mode shapes and modal stress-resultants for free circular Mindlin plates with thickness ratio $h/R = 0.10$. The number of nodal diameters is $n = 0$ (axisymmetric modes). (b) Mode shapes and modal stress-resultants for free circular Mindlin plates with thickness ratio $h/R = 0.1$. The number of nodal diameters is $n = 1, 2, 3$ and 4, respectively.

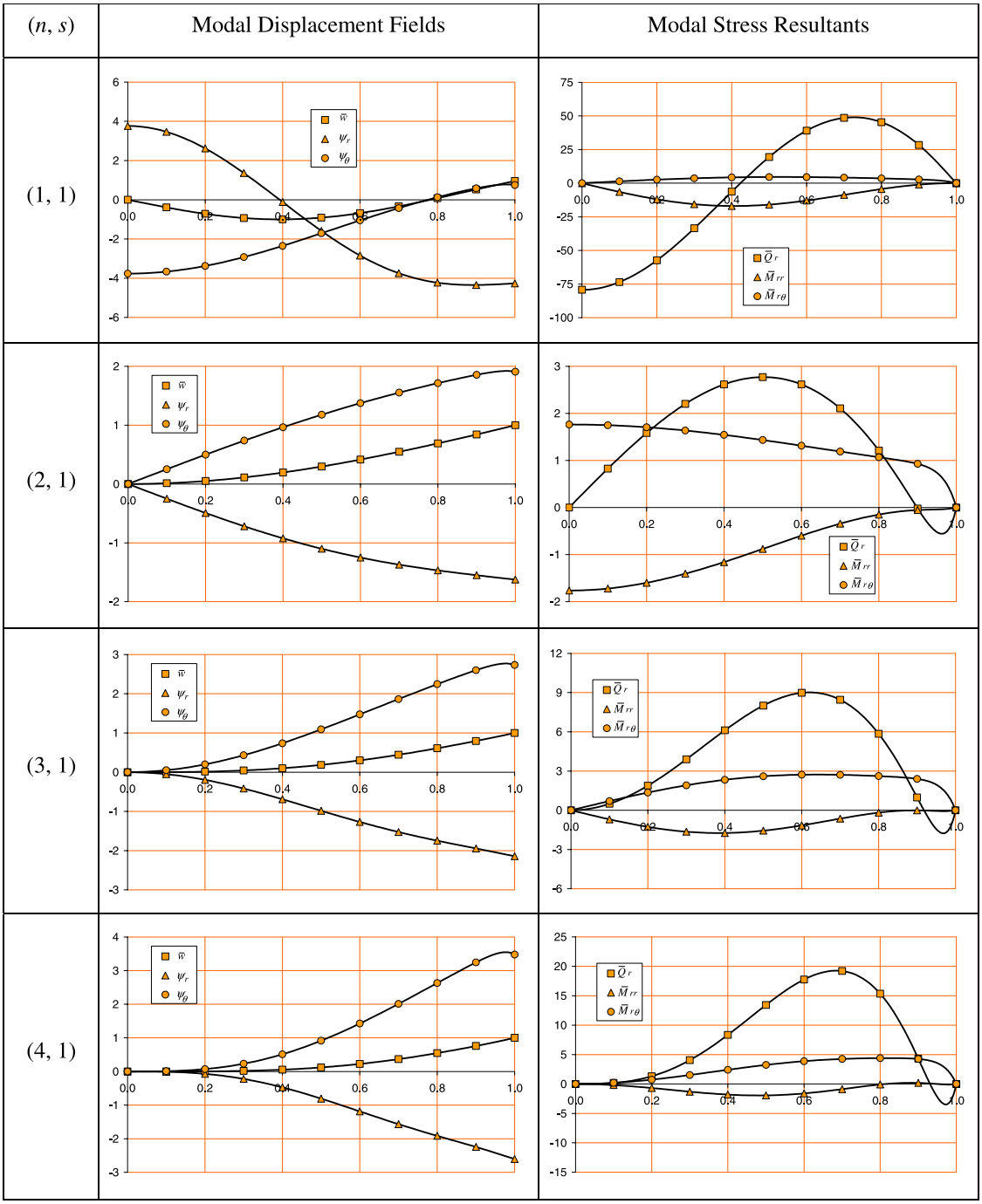

(b)

Fig. 4 (*continued*).

For the thicker plate ($h/R = 0.10$), however, the variation of the stress-resultants $\bar{Q}_r$, $\bar{M}_{rr}$ and $\bar{M}_{r\theta}$ near the vicinity of the free edge becomes quite smooth (see Figs. 4b and c) and the peak values of the shear force $\bar{Q}_r$ near the free edge for the thicker plate is much smaller than the ones for the thinner plate.

Tables 2 and 3 present the peak values and the corresponding locations of the modal displacement fields and modal stress-resultants for selected cases. These exact peak values are valuable for checking the convergence and accuracy of numerical approaches for analysing the vibration of Mindlin plates.

Fig. 5 presents the modal displacement $\bar{w}$ and the modal stress-resultants $\bar{Q}_r$, $\bar{M}_{rr}$ and $\bar{M}_{r\theta}$ for a free circular Mindlin plate obtained by the present analytical method and the p-Ritz method [12]. The plate thickness ratio h/R is taken to be 0.01 and the number of nodal diameters n and the mode sequence s are set to be 4 and 1, respectively. The number of polynomial terms in the Ritz solution is taken to be 16 [12]. The frequency parameter λ from the p-Ritz method is 21.8074 which is very close to the one from the analytical method ($\lambda = 21.7983$). It is observed that the modal displacement $\bar{w}$ from the p-Ritz method and the analytical method is almost identical. However, the modal stress-resultant $\bar{Q}_r$ from both methods shows large discrepancies. The p-Ritz stress-resultants $\bar{Q}_r$ and $\bar{M}_{r\theta}$ do not satisfy the free edge conditions. The p-Ritz shear force $\bar{Q}_r$ oscillates about the exact solution as the radial co-ordinate χ varies, and the values of Ritz $\bar{Q}_r$ are erroneous near the centre of the plate. All Ritz stress-resultants $\bar{Q}_r$, $\bar{M}_{rr}$ and $\bar{M}_{r\theta}$ become very large when the radial co-ordinate χ approaches the plate centre ($\chi \to 0$).

Fig. 6 compares the exact modal displacement $\bar{w}$ and modal stress-resultants $\bar{Q}_r$, $\bar{M}_{rr}$ and $\bar{M}_{r\theta}$ for a free circular plate obtained on the basis of the classical thin plate theory [13] and of the Mindlin plate theory. The normalized effective shear force $\bar{V}_r$ is calculated based on its definition in the classical thin plate theory and is also shown in Fig. 6. The plate thickness ratio h/R is taken to be 0.01 and the number of nodal diameters n and the mode sequence s are set to be 4 and 1, respectively. It is observed that the modal displacements $\bar{w}$ from the thin and thick plate theories are almost the same. The modal stress-resultants from both theories are also close to each other except for $\bar{Q}_r$ and $\bar{M}_{r\theta}$ near the vicinity of the plate edge. Unfortunately, the discrepancies found at the vicinity of the free edge also contain the peak values of the stress-resultants. Clearly, the natural boundary conditions, i.e., $\bar{Q}_r = 0$ and $\bar{M}_{r\theta} = 0$, are not satisfied when using the classical thin plate theory. This is due to the fact that the free edge conditions for a circular plate based on the thin plate theory are $\bar{V}_r = 0$ and $\bar{M}_{rr} = 0$ [14]. When such thin plate modal stress-resultants are used for the hydrodynamic analysis of VLFS, the stress-resultants obtained are invariably erroneous.

4. Concluding remarks

We have presented herein the exact vibration solutions, including the modal stress-resultants, of a circular Mindlin plate with free edge. The results displayed include exact peak values of modal stress-resultants which are difficult to obtain using numerical methods. Comparison of these peak values obtained using the classical thin plate theory and the Mindlin plate theory show significant differences as the plate thickness increases and as the plate vibrates at higher modes. The exact free vibration solutions when employed in the hydroelastic analysis will yield highly accurate

Table 2
The peak values and the corresponding locations of the modal displacement fields for free circular Mindlin plates

h/R	n	s	Locations and peak values of modal displacement fields											
			χ	$\bar{w}_{max}$	χ	$\bar{w}_{min}$	χ	$\psi_{r\,max}$	χ	$\psi_{r\,max}$	χ	$\psi_{\theta\,max}$	χ	$\psi_{r\,min}$
0.01	0	1	1	0.742110	0	−1	0	0	0.745	−2.36273	—	—	—	—
	0	2	0	1	0.609	−0.371550	0.291	3.56484	0.939	−2.91260	—	—	—	—
	0	3	0.409	0.404079	0	−1	0.564	3.19239	0.200	−5.43747	—	—	—	—
	0	4	0	1	0.309	−0.402400	0.146	7.25302	0.427	−4.31669	—	—	—	—
	1	1	1	0.971399	0.391	−1	0	3.98660	0.882	−4.48217	0.998	0.953097	0	−3.98660
	2	1	1	1	0	0	0	0	1	−1.61449	0.998	1.99329	0	0
	3	1	1	1	0	0	0	0	1	−2.11540	0.998	2.98159	0	0
	4	1	1	1	0	0	0	0	1	−2.56224	0.998	3.96533	0	0
0.10	0	1	1	0.738124	0	−1	0	0	0.745	−2.32455	—	—	—	—
	0	2	0	1	0.609	−0.368346	0.291	3.21354	0.943	−2.71918	—	—	—	—
	0	3	0.409	0.405187	0	−1	0.564	2.56010	0.200	−4.41299	—	—	—	—
	0	4	0	1	0.309	−0.402123	0.145	5.16760	0.986	−3.27188	—	—	—	—
	1	1	1	0.95898	0.391	−1	0	3.76390	0.891	−4.34510	0.979	0.781953	0	−3.76390
	2	1	1	1	0	0	0	0	1	−1.62462	0.978	1.92111	0	0
	3	1	1	1	0	0	0	0	1	−2.14105	0.977	2.77123	0	0
	4	1	1	1	0	0	0	0	1	−2.60297	0.977	3.54901	0	0

Note: n is the number of nodal diameters of the mode and s is the mode sequence for a given n value.

Table 3
Peak values and corresponding locations of the modal stress-resultants for free circular Mindlin plates

h/R	n	s	Locations and peak values of modal stress-resultants											
			χ	$\bar{Q}_{r\,max}$	χ	$\bar{Q}_{r\,min}$	χ	$\bar{M}_{rr\,max}$	χ	$\bar{M}_{rr\,min}$	χ	$\bar{M}_{r\theta\,max}$	χ	$\bar{M}_{r\theta\,min}$
0.01	0	1	0.536	14.0887	1	0	0.962	0.038757	0	−6.94744	—	—	—	—
	0	2	0.827	59.9881	0.300	−139.090	0	24.8036	0.591	−16.5590	—	—	—	—
	0	3	0.200	476.498	0.573	−287.098	0.391	35.8292	0	−56.9108	—	—	—	—
	0	4	0.427	675.347	0.145	−1135.98	0	101.479	0.291	−64.0755	—	—	—	—
	1	1	0.727	53.4462	0	−84.7962	0.979	0.067716	0.400	−17.8019	0.527	4.85809	0	0
	2	1	0.509	2.95972	0.990	−1.45690	0.9273	0.034262	0	−1.78985	0	1.78985	1	0
	3	1	0.627	10.0444	0.990	−5.74364	0.900	0.316567	0.373	−1.77989	0.618	2.77810	0	0
	4	1	0.691	22.4744	0.991	−13.8572	0.891	0.958030	0.464	−2.01492	0.764	4.43478	0	0
0.10	0	1	0.536	13.6593	1	0	0.964	0.033507	0	−6.82216	—	—	—	—
	0	2	0.818	51.6316	0.300	−122.608	0	22.4005	0.591	−15.1111	—	—	—	—
	0	3	0.200	365.435	0.573	−222.106	0.382	29.0071	0	−46.2034	—	—	—	—
	0	4	0.427	440.725	0.145	−742.776	0	72.3533	0.291	−45.7085	—	—	—	—
	1	1	0.727	49.0370	0	−79.2851	0.992	0.007382	0.409	−16.9500	0.527	4.62564	1	0
	2	1	0.500	2.77106	0.963	−0.557011	1	0	0	−1.76356	0	1.76356	1	0
	3	1	0.618	9.01726	0.968	−1.76381	0	0	0.382	−1.74232	0.636	2.73075	1	0
	4	1	0.682	19.2668	0.973	−3.47288	0.882	0.196978	0.482	−1.95099	0.818	4.39324	1	0

Note: n is the number of nodal diameters of the mode and s is the mode sequence for a given n value.

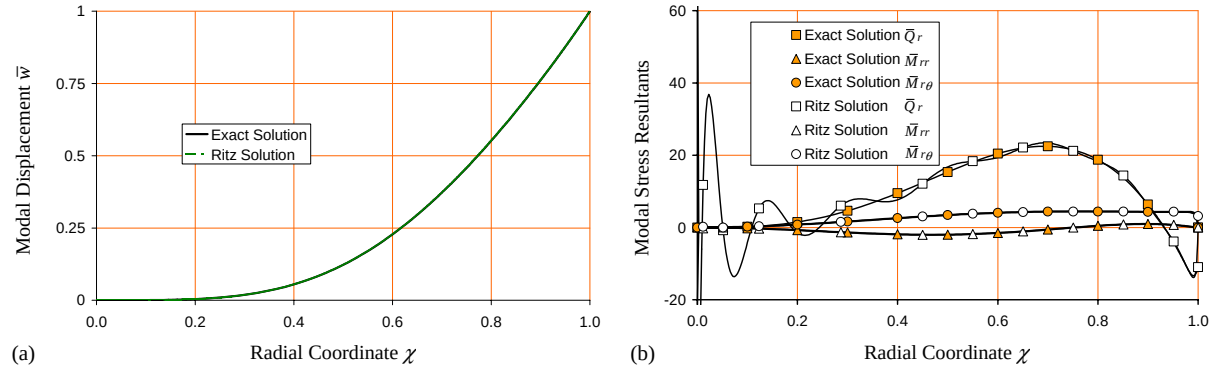

Fig. 5. Mode shapes and modal stress-resultants in the radial direction for free circular Mindlin plates by the analytical method and the p-Ritz method ($h/R = 0.01$, $n = 4$, $s = 1$). (a) Modal displacement $\bar{w}$ and (b) modal stress-resultants.

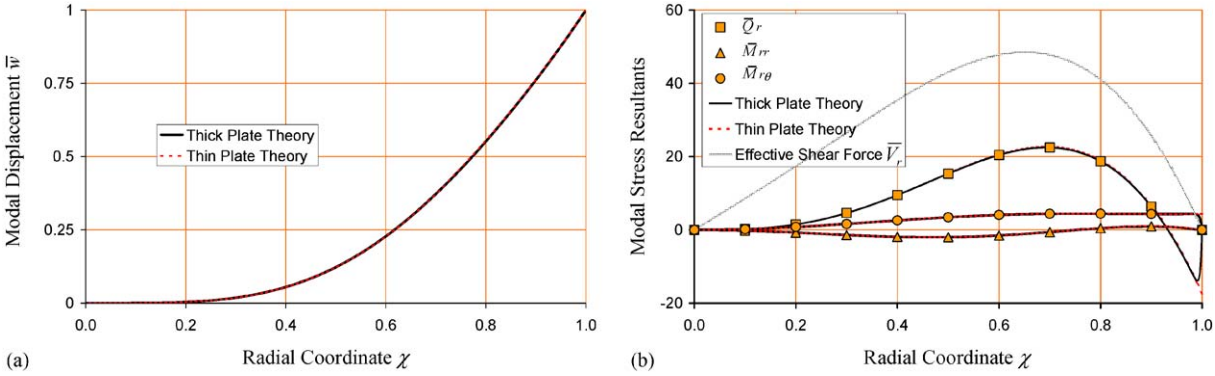

Fig. 6. Mode shapes and modal stress-resultants in the radial direction for free circular plates based on classical thin plate theory and Mindlin plate theory ($h/R = 0.01$, $n = 4$, $s = 1$). (a) Modal displacement $\bar{w}$ and (b) modal stress-resultants.

deflections and stress-resultants of circular VLFS under the action of waves as reported in a recent paper [14]. The availability of such benchmark hydroelastic responses of VLFS will be extremely useful to engineers and researchers who are developing numerical techniques for the hydroelastic analysis of arbitrarily shaped VLFS.

Acknowledgements

The second author is very grateful to Prof. C.M. Wang for the invitation to visit the Department of Civil Engineering of the National University of Singapore and to conduct this joint research work. The financial assistance from NUS Research Grant R-264-000-111-112 is greatly appreciated.

References

[1] M. Takaki, X. Gu, On motion performance of a huge floating structure in waves, *Proceedings of the International Workshop on Very Large Floating Structures*, Hayama, Kanagawa, Japan, November 25–28, 1996, pp. 157–164.

[2] M. Kashiwagi, A new solution method for hydroelastic problems of a very large floating structure in waves, *Proceedings of the* 17*th International Conference on Offshore Mechanics and Artic Engineering*, *American Society of Mechanical Engineers*, Lisbon, Portugal, OMAE98-4332, July 8.

[3] T. Utsunomiya, E. Watanabe, R. Eatock Taylor, Wave response analysis of a box-like VLFS close to a breakwater. *Proceedings of the* 17*th International Conference on Offshore Mechanics and Artic Engineering*, *American Society of Mechanical Engineers*, Lisbon, Portugal, OMAE98-4331, 1998, pp. 1–8.

[4] C.M. Wang, Y. Xiang, T. Utsunomiya, E. Watanabe, Evaluation of modal stress-resultants in freely vibrating plates, *International Journal of Solids and Structures* 38 (2001) 6525–6558.

[5] Y. Xiang, C.M. Wang, T. Utsunomiya, C. Machimdamrong, Benchmark stress-resultant distributions for vibrating rectangular plates with two opposite edges free, *Journal of Computational Structural Engineering* 1 (1) (2001) 49–57.

[6] C.M. Wang, Y.C. Wang, J.N. Reddy, V. Thevendran, Improved computation of stress-resultants in the *p*-Ritz method, *Journal of Structural Engineering, American Society of Civil Engineers* 128 (2) (2002) 249–257.

[7] C.M. Wang, Y.C. Wang, J.N. Reddy, Problems and remedy for the Ritz method in determining stress-resultants of corner supported rectangular plates, *Computers and Structures* 80 (2) (2002) 145–154.

[8] R.D. Mindlin, H. Deresiewicz, Thickness-shear and flexural vibrations of a circular disk, *Journal of Applied Physics* 25 (1954) 1329–1332.

[9] T. Irie, G. Yamada, K. Takagi, Natural frequencies of thick annular plates, *Journal of Applied Mechanics, American Society of Mechanical Engineers* 49 (1982) 633–638.

[10] R.D. Mindlin, Influence of rotatory inertia and shear on flexural motions of isotropic, elastic plates, *Journal of Applied Mechanics, American Society of Mechanical Engineers* 18 (1951) 31–38.

[11] Y. Xiang, Exact vibration solutions for circular Mindlin plates with multiple concentric ring supports, *International Journal of Solids and Structures* 39 (2002) 6081–6102.

[12] K.M. Liew, Y. Xiang, C.M. Wang, S. Kitipornchai, *Vibration of Mindlin Plates: Programming the p-Version Ritz Method*, Elsevier Science, Oxford, UK, 1998.

[13] A.W. Leissa, *Vibration of Plates*, NASA SP-169, Office of Technology Utilization, Washington, 1969.

[14] E. Watanabe, T. Utsunomiya, C.M. Wang, Y. Xiang, Hydroelastic analysis of Pontoon-Type circular VLFS, in: J.S. Chung, S. Prinsenberg (Eds.), *Proceedings of the* 13*th Offshore and Polar Engineering Conference*, Honolulu, Hawaii, May 25–30, 2003, Vol. I, International Society of Offshore and Polar Engineers, Cupertino, CA, 2003, pp. 93–99.